Transactions, SMiRT-23
Manchester, United Kingdom - August 10-14, 2015
Division II

MEASUREMENTS OF STRESS CONCENTRATION BEHAVIOUR IN AGR NUCLEAR GRAPHITE

Matthew S. L. Jordan [1a], Luis Saucedo-Mora[1], Selim Barhli[1], David Nowell[2], and T. James Marrow[1]

[1] Department of Materials, University of Oxford, UK
[2] Department of Engineering, University of Oxford, UK

[a]matthew.jordan@materials.ox.ac.uk

ABSTRACT

The UK advanced gas-cooled reactor (AGR) nuclear power stations are graphite moderated. Throughout reactor life, fast neutron irradiation and radiolytic-oxidation increase the risk of cracking in graphite components from the stress-concentrating keyways. Forward predictions of reactor integrity require knowledge of the strengths of in-service components, which are estimated from data that includes the flexural strength of reactor-extracted specimens and notched feature tests of non-irradiated graphite. The notch sensitivity of irradiated graphite is not monitored at present; knowledge of this parameter would increase confidence in the conservatism of the current assessments. This work is part of a project that aims to quantify the effects of loading mode and geometry on notch sensitivity, with the objective of developing a measurement methodology for small test specimens.

The deformation fields ahead of wedge-loaded keyhole-shaped notches specimens of non-irradiated Gilsocarbon have been quantified by *in situ* synchrotron X-ray computed tomography (XCT), analysed by digital volume correlation (DVC), and compared with finite element (FE) simulations with experimentally accurate boundary conditions. Deviations from linear-elasticity were mapped to investigate non-linear damage development ahead of blunt and sharp features, with the aim of quantifying the damage-law for non-irradiated graphite. Heterogeneous behaviour was observed between the microstructural phases, but no significant concerted non-linear deformation at the notch tip prior to failure. The developed techniques will be used to study damage development in notched four-point bend testing of small Gilsocarbon samples.

INTRODUCTION

Between 1976 and 1989, the UK brought online fourteen nuclear power stations of the Advanced Gas-Cooled Reactors (AGR) design. Graphite bricks and CO_2 were chosen as the moderator and coolant, respectively; the fuel and control rods are accommodated in an array of vertical channels formed by large Gilsocarbon graphite bricks. The continuous fast neutron bombardment and radiolytic oxidation cause significant changes to the graphite (Marsden and Hall (2012)), including the potentially life-limiting phenomenon of 'keyway-root cracking'; due to irradiation-induced dimension change, tensile hoop stresses evolve on surfaces containing keyway slots in the bricks' external surface. Graphite's sensitivity to these stress raisers would encourage crack initiation (hence, 'keyway-root cracking') and subsequent brick distortion, which may have implications for the fuel and control rod movement.

Figure 1 indicates the medium to coarse, polygranular and heterogeneous microstructure of Gilsocarbon, with spherical 'filler particles' of up to 1 mm diameter held in a porous matrix; graphite crystals a few microns in size are observed in both phases and pore sizes span the nano- to millimetre length-scales (Nightingale (1963)). Under applied stresses, Gilsocarbon is near isotropic, while irradiation results in increasingly linear stress-strain behaviour (Bell *et al.* (1962), Best *et al.* (1985), Taylor *et al.* (1967)).

Improving the confidence of prediction of keyway-root cracking will require both an understanding of how the microstructure affects the ability to accommodate plastic strain ahead of a stress concentrator, and a method for monitoring the reactor component notch sensitivity evolution with radiolytic-oxidation. The material that may be extracted from reactors is necessarily limited; the effects of irradiation and oxidation on the stiffness and strength of reactor graphite are measured from small (centimetre scale) un-notched flexural specimens. No methodology exists for notch sensitivity measurement with this volume of material.

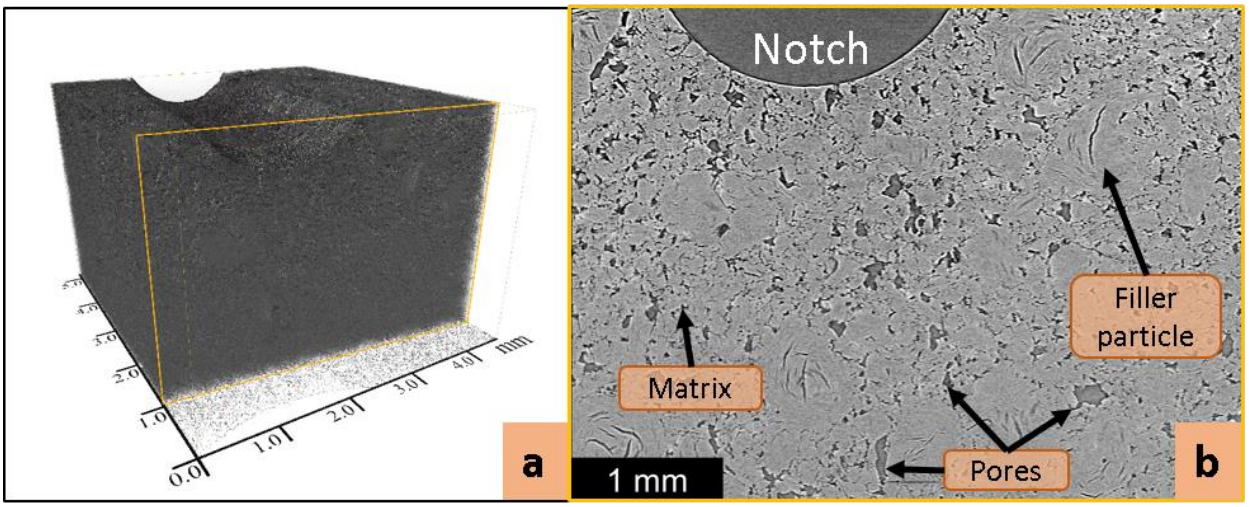

Figure 1: 2 mm sample XCT: (a) 3-D reconstruction, with slice perpendicular to notch axis, (orange outline); (b) microstructural features indicated on projected slice.

For homogeneous media, geometric stress concentrations are readily predicted in engineering simulations, by finite element (FE) modelling for example. However, the effects of stress and strain gradients on Gilsocarbon strength are not fully described in a general model (Brocklehurst, J.E. and Brown (1973), Tucker *et al.* (1986)). Similar to other graphite grades, non-irradiated Gilsocarbon behaves as if un-notched for notches of diameter or depth less than about 1 mm (Brown *et al.* (1986), Burchell (1996)). Though no reported experimental work conclusively supports it, the notch insensitivity to small notches is attributed to the microstructural defect or pore size (Brocklehurst, J. E. and Darby (1974), Hodgkins (2006), Marshall and Priddle (1973)). In terms of fracture, due to the ability to accommodate limited plastic strain prior to a 'graceful' failure, Gilsocarbon is termed a 'quasi-brittle' material. The mechanism and distribution of non-linear straining is an open research question; 'plastic zone' formation is a potential mechanism, whereby regions of the material fail in a concerted manner as some yield criterion is exceeded. Fracture propagation studies provide observations from which the presence and size (several millimetres) of a 'damage' zone has been inferred (Hodgkins *et al.* (2006), Hodgkins *et al.* (2007), Mostafavi *et al.* (2013a), Ouagne *et al.* (2004)).

The analysis of a small specimen test for notch sensitivity would be complicated by either the damage zone strongly interacting with sample boundaries (analogous to the effects of plasticity in metals), or scale dependent damage due to the microstructure. This work presents experimental observations of damage during crack initiation ahead of blunt features in Gilsocarbon. Up until fracture was detected, samples with keyhole different notch radii were progressively loaded by wedge-compression. *In situ* imaging was made during loading by non-destructive, region-of-interest synchrotron X-ray Computed Tomographs (XCTs) and single exposure radiographs, with digital image correlation (DIC) and digital volume correlation (DVC) employed for the quantitative analyses.

EXPERIMENTAL

Blunt stress raisers were simulated by wire-eroding (for minimal mechanical damage) keyhole notches with tip diameters of 2 and 4 mm in test specimens of Graftech (formerly UCAR) manufactured IM1-24 Gilsocarbon (moulded GCMB grade) polygranular nuclear graphite. Using a tension/compression rig loaned from the University of Birmingham, a 10° wedge was inserted into the sample under quasi-static conditions to progressively higher peak loads, until a drop in load with increasing displacement was observed (a 'pop-in'). A bespoke jig permitted visual three-dimensional positioning of the sample below the wedge, with a fine self-alignment achieved by two degrees of freedom: free rotation of the wedge and one-dimensional sample translation. An initial central alignment was achieved by gently adjusting the sample position under a 10 N pre-load (displacement controlled) to attain a minimum reaction force. The peak loads were measured in preliminary testing of seven samples of each sample geometry. The rig measured wedge displacements and reaction loads to accuracies of 1 μm and 1 N, respectively.

Testing of one sample of each notch tip diameter was conducted as part of experiment EE8519-1 on beam line I12 at the Diamond Light Source (DLS; Drakopoulos *et al.* (2015)). Radiographs (single exposure X-ray absorption maps, with the beam aligned parallel to the notch direction; Figure 2a) were collected at 10 N intervals to monitor the notch opening behaviour; at 4.8 μm.pixel^{-1} resolution, the radiograph field of view was 12 x 16 mm. In the periodically loaded and fully unloaded states, X-ray computed tomographs (XCTs) were collected. Radiograph and tomographic projection exposure times of approximately 0.5 s and 2 s, respectively, using an X-ray energy of 53 keV. The tomographs yielded virtual microstructure images (Figure 1) reconstructed using the Manchester Back-filtered Projection algorithm, as implemented at the DLS. The XCTs had a cubic voxel, or three-dimensional pixel, resolution of 1.8 μm and approximate maximum dimensions of 7 x 7 x 5 mm and 7 x 7 x 3.5 mm for the 2 mm and 4 mm diameter notches, respectively; the smaller 4 mm volume was due to a gradual optic degradation during the experiment that increased noise in the lower part of the radiograph, remote from the notch.

The heterogeneous porous microstructure absorbs X-rays differentially, resulting in contrast features in the radiographs (two-dimensional, 2-D) and reconstructed tomographs (three-dimensional, 3-D) that can be tracked using non-contact, non-destructive Digital Image Correlation (DIC) techniques; the 3-D version referred to as Digital Volume Correlation (DVC). Both techniques have been used extensively in the study of fracture mechanics (for example, Bay *et al.* (1999), Becker *et al.* (2011), Mostafavi *et al.* (2013b), Sánchez-Arévalo and Pulos (2008), Triconnet *et al.* (2009)). 3-D displacement fields of the notch tip were generated from DVC analysis of the tomographs, while the notch opening behaviour was measured from DIC of the larger field of view 2-D radiographs; LaVision's *DaVis* (version 8) software was used for all image correlation operations. Correlations of 1024^3 voxels tomographic sub-volumes for a sample under a rigid body translation of 10 μm were used for selecting the DVC settings; the resultant sensitivity (the minimum resolvable displacement) was evaluated as the standard deviation of the displacement.

RESULTS

Figure 3 shows horizontal slices immediately ahead of the notch tips for both samples from the tomographs pre- and post-failure for each of the DLS-tested samples. In both cases, after peak load, a full-width crack was observed at the notch tip (Figures 3b and d). The 4 mm sample fractured in the final 10 % of the loading – no macroscopic cracking was present at 90 % peak load (85 N, Figure 3c). In the 2 mm sample, while no cracking was evident at 64 % peak load (50 N), an approximately third-width crack had developed by 96 % peak load (75 N, Figure 3a). The peak load distributions for preliminary sets of seven samples and the individual samples tested at the DLS are summarised in Table 1. The pop-in load drop was less than 15 N in each case.

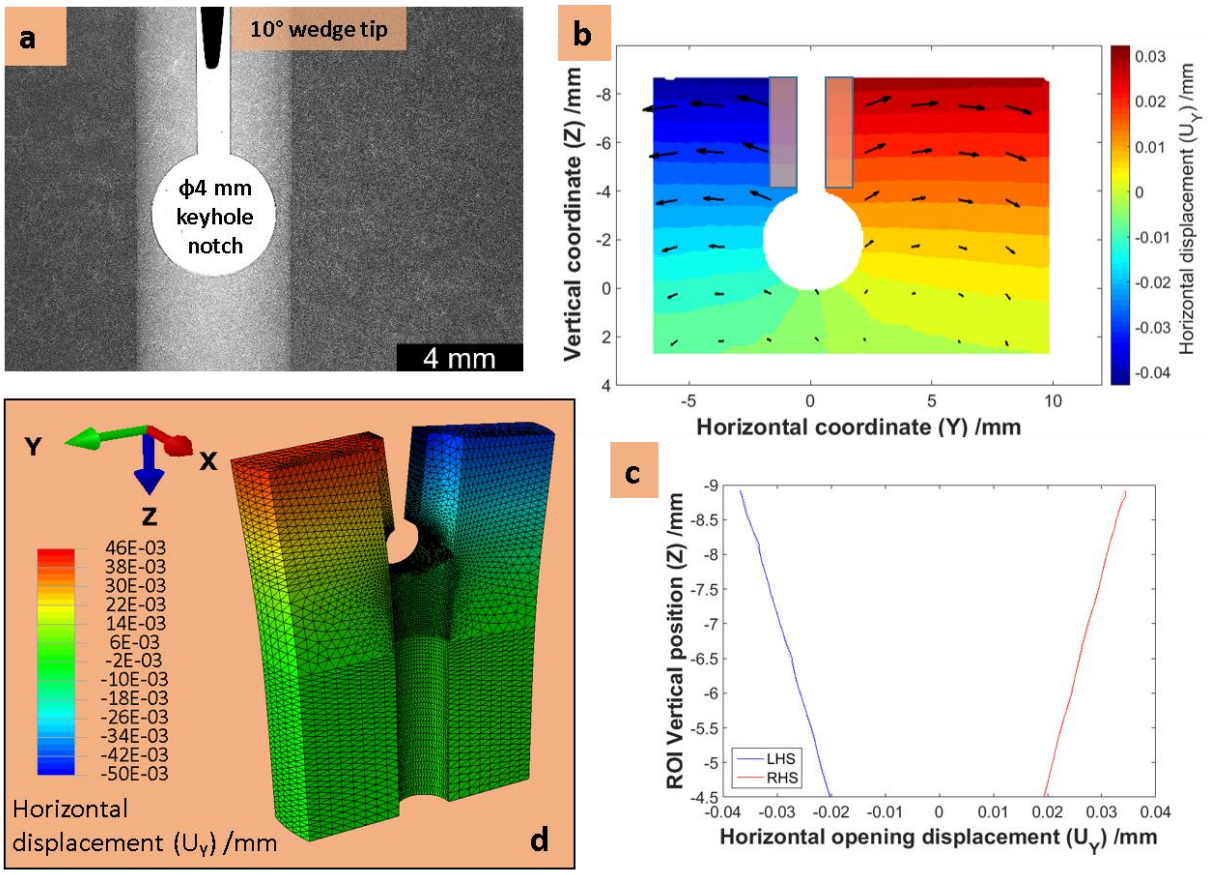

Figure 2: FE simulation: (a) example radiograph corrected for beam variation, (b) radiograph DIC (vectors: subset of scaled 2-D displacements, colour map: horizontal displacement component). For the regions of interest (ROI) highlighted in orange on (b), linear fits to the displacements (c) are applied as boundary conditions on the left and right hand side of the notch face (LHS and RHS, respectively) in the half-symmetry FE model (d).

Table 1 – Peak load distributions for preliminary testing (average ± standard deviation (SD) of seven samples) compared with the samples tested at the DLS.

Notch tip geometry	Preliminary tests: Peak Load (N)	Peak Load at DLS (N)
2 mm	90 ± 11	78 (-1.1 SD from mean)
4 mm	94 ± 11	95 (+0.1 SD from mean)

To prepare for DVC, the loading sequence tomographs were manually registered against the pre-loaded reference state and cropped to remove image edge artefacts. A DVC sensitivity of 0.2 µm at a 30 µm spatial distance between displacement vectors of was achieved using a multi-pass correlation scheme with the finest interrogation volume of 128^3 voxels and 75 % overlap, evaluated as the best compromise of precision and resolution. Output displacement fields were corrected for rigid body motions (RBM) including displacement and rotation, following a method based on that by Mostafavi *et al.* (2015). For representative microstructural regions (for the locations indicated in Figure 3, vertical slices are presented in Figure 4), DVC displacements are presented in Figure 5.

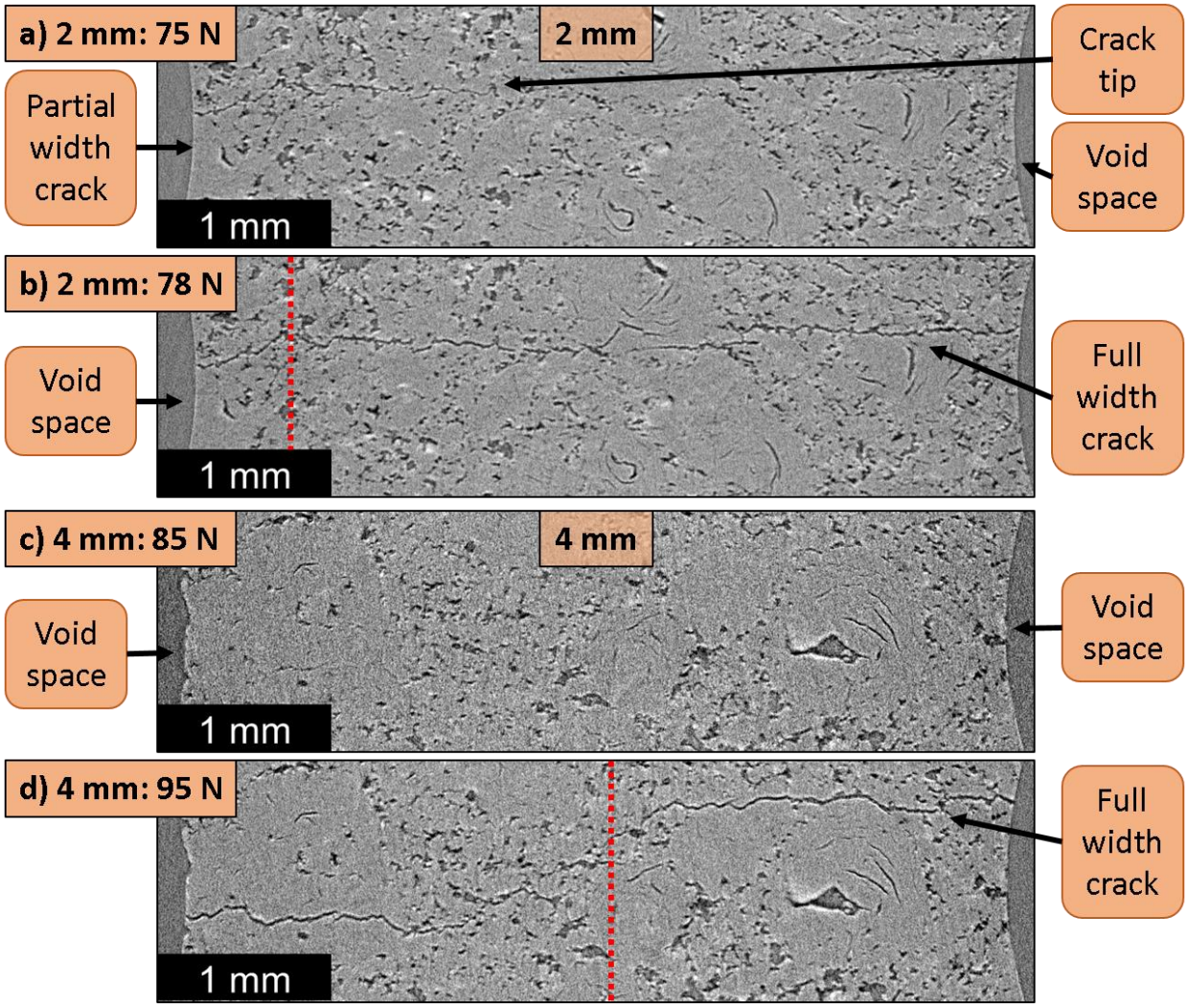

Figure 3: Virtual microstructure horizontal slices from tomographs at loads before and after peak failure in the 2mm sample: (a) 75 N (partial cracking) and (b) 78 N (full-width crack), and the 4 mm sample: (c) 85 N (no crack is visible) and (d) 95 N (full-width crack). The slices are immediately ahead of the respective notch tips. The red dotted lines indicate the vertical slice locations shown in Figures 4 and 5.

Measured by the radiograph DIC (Figure 2b), the pressure of the wedge caused linear horizontal (Figure 2c) and vertical displacements along the notch faces. Note that while sample compression caused the sample centre to move downwards, the motion appears towards the wedge when displayed relative to the notch tip, as in (Figure 2b). The predicted linear elastic displacements of the samples were simulated in Simulia's *Abaqus*, as a half-symmetry geometry FE model meshed in quadratic tetrahedral elements with refinement about the notch tip (Figure 2d). Elastic properties for Gilsocarbon were chosen to agree with Preston, S.D. (1988), Preston, S. D. and Marsden (2006): Young's Modulus, E = 12 GPa and Poisson ratio, ν = 0.22. Displacement boundary conditions along the notch were prescribed as the fitted linear behaviour for the regions indicated on Figure 2b, so that the simulation mimicked the experimental loading. An exact *ab initio* simulation would have required a full description of the frictional contact between wedge and sample, damage of the notch faces and any slight wedge-sample misalignments with a high risk of calculating a non-representative strain field.

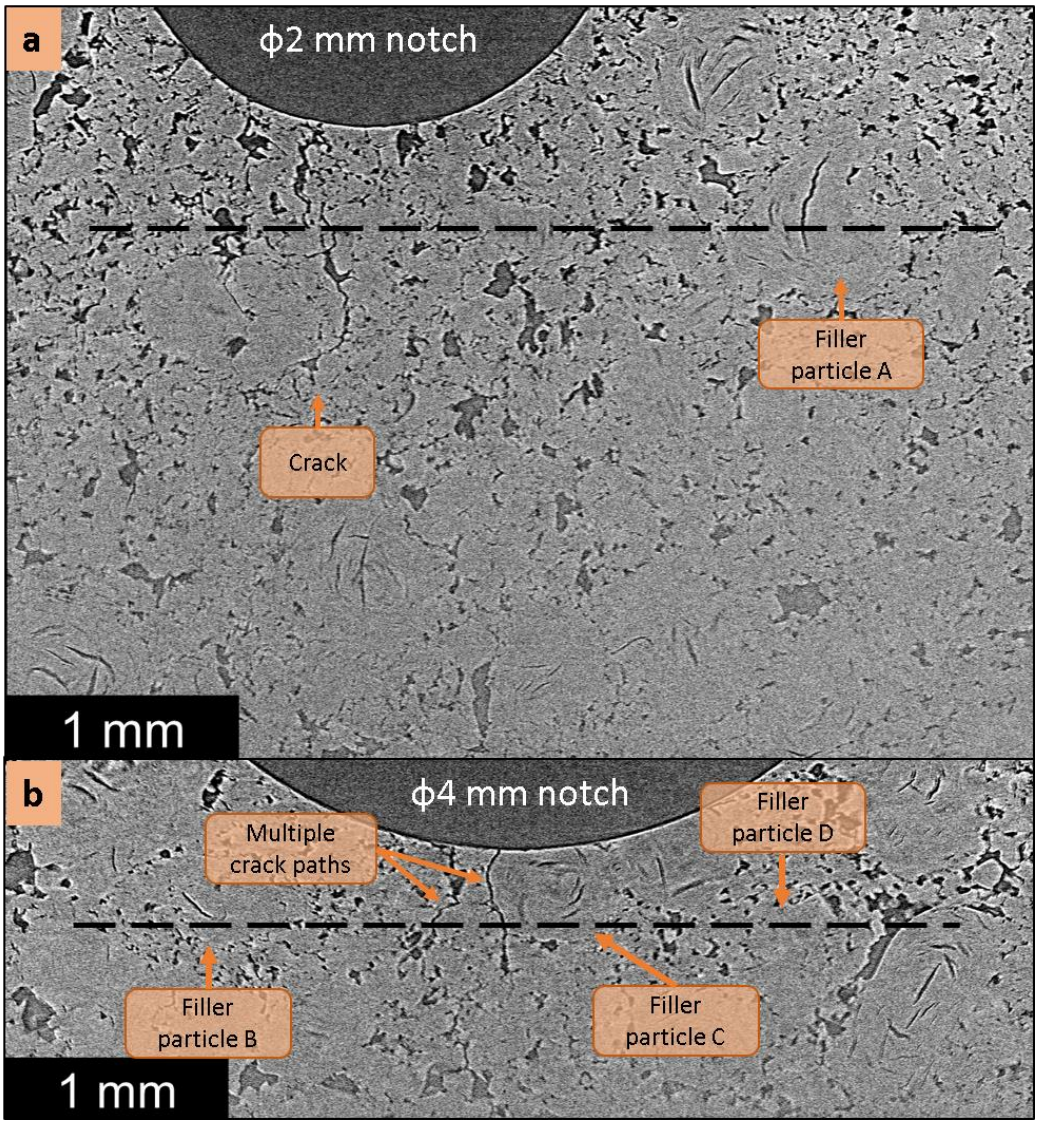

Figure 4: Microstructure slices perpendicular to notch axis in cracked samples with (a) 2 mm notch tip (contrast with Figure 1b) and (b) 4 mm notch tip, for the locations indicated on Figure 3. Black dashed lines are the profile paths, and the labels relate to features in Figures 5 and 6.

Displayed relative to the notch tips (Figure 5), the DVC notch opening displacements increased continuously with distance from the notch to ± 3.5 µm and ± 5 µm at the tomograph edges, for the 2 and 4 mm samples respectively. The differences in the measured and expected displacements were quantified as 'Deviation' fields (experimental – simulated, Figure 5), calculated following a notch tip registration of the FE displacements and interpolation to the DVC vector spatial positions using a neural network algorithm (Wendland (2004)). Figure 6 shows lines profiles extracted from the Figure 5 maps. Significant fluctuations, around 1.2 µm and increasing with applied load, were observed, generally not contacting the notch but tending to be localised about filler particle positions. The appearance of macro-cracking was evident as a Deviation step change of greater magnitude than the background (microstructural) variation, of highest gradient in the crack vicinity. The cracked microstructural images (Figures 3d and 4), show multiple crack paths formed in the 4 mm notch tip specimen. Unlike the narrow path highlighted in the DVC and Deviation 2 mm notch sample maps (Figure 5), the 4 mm notch maps have a broader discontinuity observed post cracking, and a "two-step" discontinuity in Figure 6, that reflects the multiple crack paths.

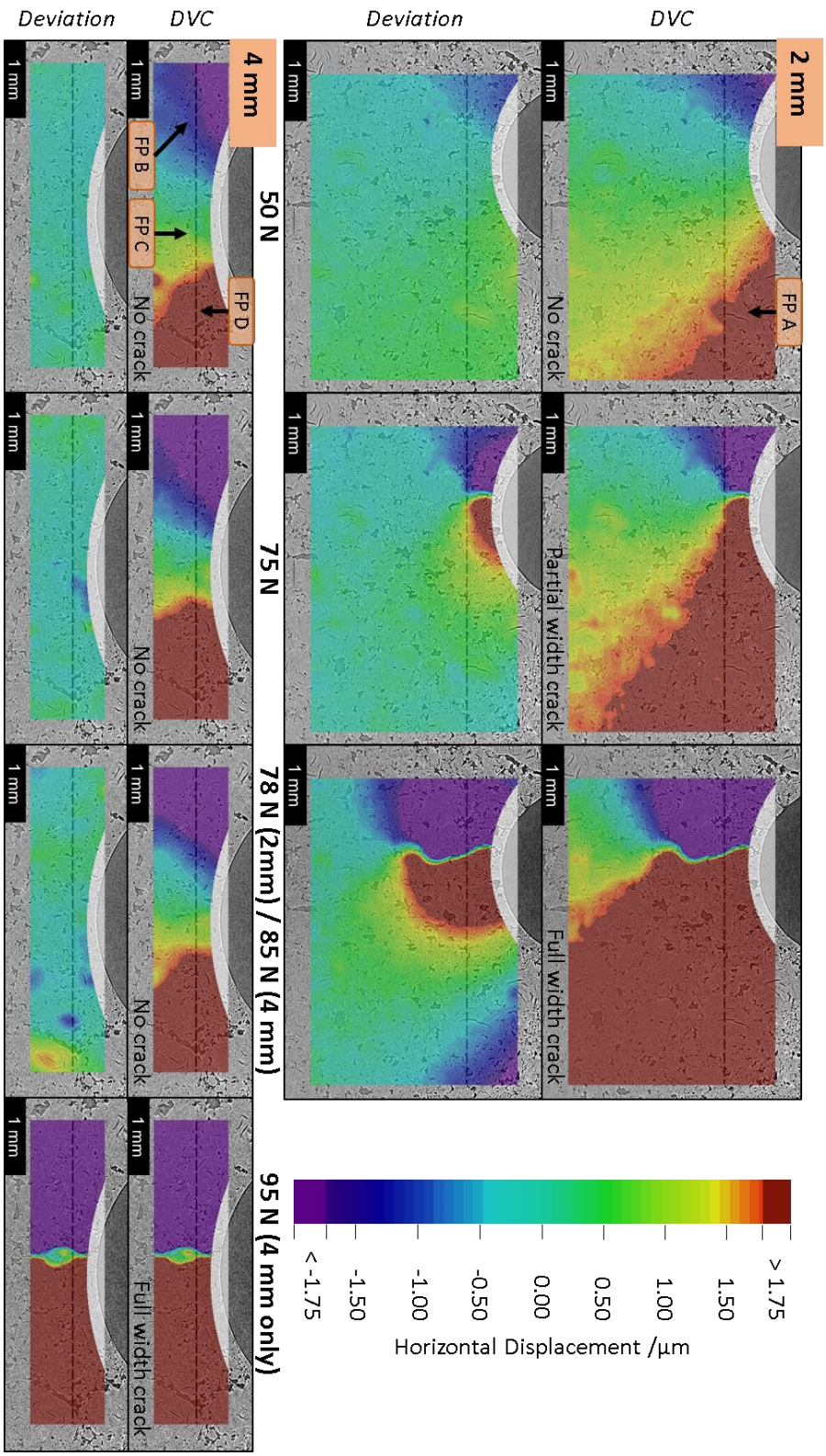

Figure 5: *(rotated)* Loading displacements for the samples as DVC and Deviation maps, for the slices in Figure 4. Annotations and dashed black lines indicating profile paths are *as per* Figures 4 and 6 (label FP = filler particle).

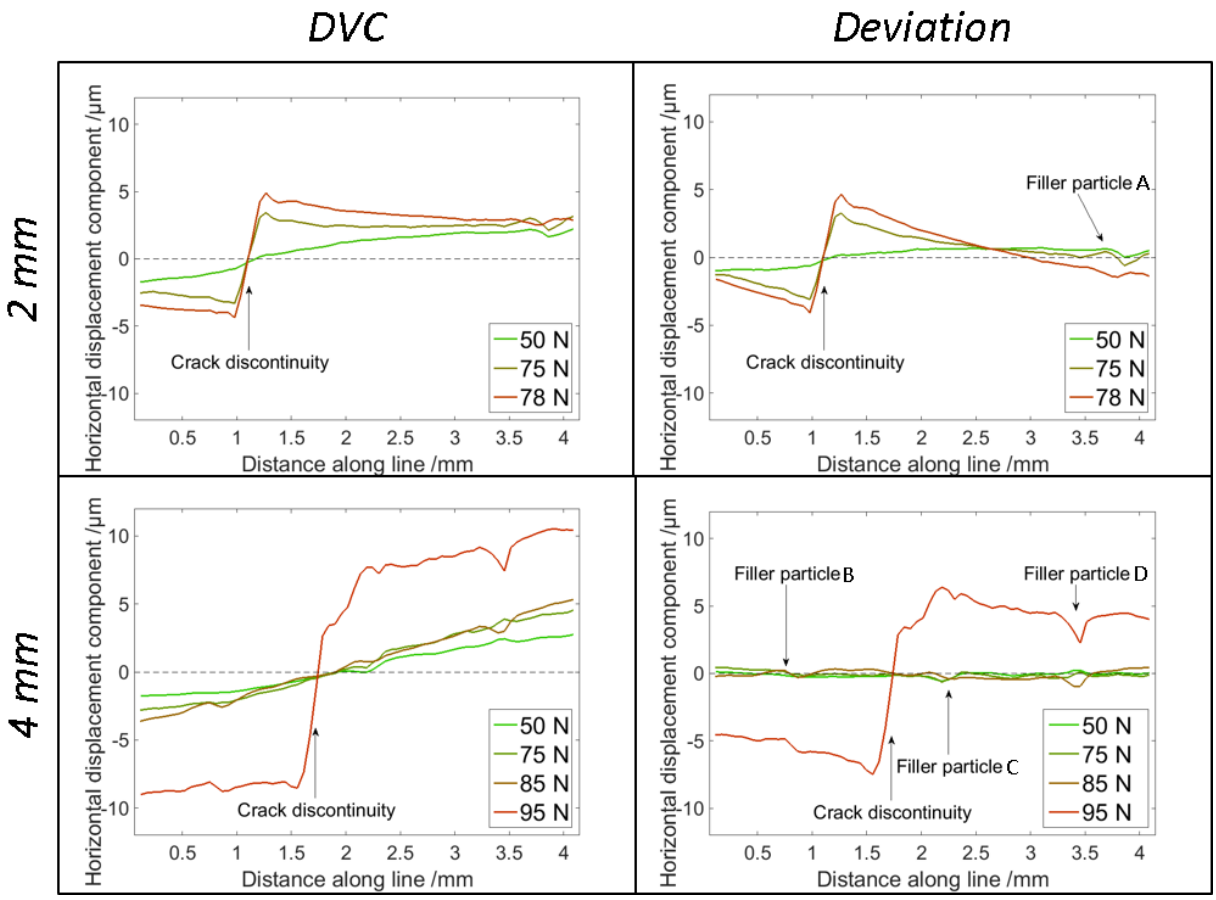

Figure 6: Line profiles indicating Gilsocarbon's heterogeneous behaviour for the paths and labels shown in Figures 4 and 5.

DISCUSSION

The tomography indicates that the peak load corresponds to full-width fracture and a subsequent softening of the specimen's compliance, and Table 1 demonstrates that the 2 mm geometry is the weaker, in accordance with the sharper stress concentrator. Figure 3a reveals that partial-width macro-crack nucleation occurred in the 2 mm sample before the peak load, and may be the cause of the statistically low peak load. The propagated cracks preferentially include pores, as observed by visually tracing the crack paths in Figures 3b and d; currently the hypothesis of nucleation at significant pore or defect in explanation of the low 2 mm sample strength is being explored.

The baseline Deviation variation is comparable to the DVC error (± 0.2 µm), verifying a good agreement between the FE simulations with prescribed boundary conditions and the experimental displacements, particularly in the 4 mm maps (50N to 85N; Figures 5 and 6). After full-width cracking, the FE model does not fully compensate for the change in geometry. The subtraction of the elastic displacement fields permits visualisation and quantification of heterogeneous strain variations; hot spot regions with displacements of up to 1.2 µm are generally localised on filler particles. This suggests a lower stiffness compared to the matrix possibly due to their large lenticular pores. Previous studies also observed a correlation between deformations and Gilsocarbon pores, such as the *in situ* measurements with ESPI (Electronic Speckle Pattern Interferometry) by Joyce *et al.* (2008).

Pre-cracking damage would result in non-linear strains, manifesting in the Deviation maps as large displacements. The dominant notch strain field dominates the DVC data and any damage behaviour is unclear, whereas the Deviation data confirms that Gilsocarbon deforms near the notch as if it were an elastic material, with no evidence for a significant damage region.

CONCLUSION

Crack initiation in non-irradiated Gilsocarbon nuclear graphite has been analysed to quantify Deviations from linear displacement behaviour by combining synchrotron imaging, image correlation techniques, and finite element simulation. Ahead of stress concentrating notches of 2 and 4 mm diameter, no evidence of significant inelastic deformation was observed before cracking. Microstructural scale Deviations, typically localised at filler particles, were evident.

ACKNOWLEDGEMENTS

Assistance is appreciated from M. Mostafavi, Ye. Vertyagina, C. Reinhard, K. Wanelik, R. Atwood, C. Cooper, D. Collins, S. Sun and B. Cai during experiment EE8519-1 at the Diamond Light Source. B. Connolly at the University of Birmingham kindly loaned the tomography stage. This work is sponsored by EPSRC Industrial CASE studentship 11220486, with support and materials supplied by EDF Energy. The opinions expressed in this paper are the Authors', and are not necessarily those of EDF Energy.

Bay, B. K., Smith, T. S., Fyhrie, D. P. and Saad, M. (1999), "Digital volume correlation: Three-dimensional strain mapping using X-ray tomography", *Experimental Mechanics*, 39, 217-226.

Becker, T. H., Marrow, T. J. and Tait, R. B. (2011), "Damage, crack growth and fracture characteristics of nuclear grade graphite using the Double Torsion technique", *J Nucl Mater*, 414, 32-43.

Bell, J. C., Bridge, H., Cottrell, A. H., Greenough, G. B., Reynolds, W. N. and Simmons, J. H. W. (1962), "Stored Energy in the Graphite of Power-Producing Reactors", *Philosophical Transactions of the Royal Society of London. Series A, Mathematical and Physical Sciences*, 254, 361-395.

Best, J. V., Stephen, W. J. and Wickham, A. J. (1985), "Radiolytic graphite oxidation", *Progress in Nuclear Energy*, 16, 127-178.

Brocklehurst, J. E. and Brown, R. G. (1973), "Fatigue, Notch Sensitivity and Work of Fracture Studies on Isotropic Graphite", Springfields, TRG 2513(S).

Brocklehurst, J. E. and Darby, M. I. (1974), "Concerning the fracture of graphite under different test conditions", *Materials Science and Engineering*, 16, 91-106.

Brown, R. G., Birch, M., Stainthorpe, C. and Rosen, P. (1986), "A study of the notch sensitivity and the effect of specimen size on the strength of a wide range of graphites", Springfields Nuclear Power Development Laboratories, .

Burchell, T. D. (1996), "A microstructurally based fracture model for polygranular graphites", *Carbon*, 34, 297-316.

Drakopoulos, M., Connolley, T., Reinhard, C., Atwood, R., Magdysyuk, O., Vo, N., Hart, M., Connor, L., Humphreys, B., Howell, G., Davies, S., Hill, T., Wilkin, G., Pedersen, U., Foster, A., De Maio, N., Basham, M., Yuan, F. and Wanelik, K. (2015), "I12: the Joint Engineering, Environment and Processing (JEEP) beamline at Diamond Light Source", *Journal of Synchrotron Radiation*, 22, 828-838.

Hodgkins, A. (2006), *Faculty of Engineering and physical sciences*, Doctor of Philosophy, University of Manchester, Manchester, .

Hodgkins, A., Marrow, T. J., Mummery, P., Marsden, B. and Fok, A. (2006), "X-ray tomography observation of crack propagation in nuclear graphite", *Mater Sci Tech-Lond*, 22, 1045-1051.

Hodgkins, A., Marrow, T. J., Mummery, P., Marsden, B. J. and Fok, A. S. L. (2007), "Crack propagation resistance and damage mechanisms in nuclear graphite", *Roy Soc Ch*, 127-133.

Joyce, M. R., Marrow, T. J., Mummery, P. and Marsden, B. J. (2008), "Observation of microstructure deformation and damage in nuclear graphite", *Engineering Fracture Mechanics*, 75, 3633-3645.

Marsden, B. J. and Hall, G. N. (2012), "4.11 - Graphite in Gas-Cooled Reactors", *Comprehensive Nuclear Materials*, Elsevier, Oxford, 325-390.

Marshall, P. and Priddle, E. K. (1973), "Room temperature fatigue crack propagation in reactor graphites", *Carbon*, 11, 541-546.

Mostafavi, M., Baimpas, N., Tarleton, E., Atwood, R. C., McDonald, S. A., Korsunsky, A. M. and Marrow, T. J. (2013a), "Three-dimensional crack observation, quantification and simulation in a quasi-brittle material", *Acta Materialia*, 61, 6276-6289.

Mostafavi, M., Collins, D. M., Cai, B., Bradley, R., Atwood, R. C., Reinhard, C., Jiang, X., Galano, M., Lee, P. D. and Marrow, T. J. (2015), "Yield behavior beneath hardness indentations in ductile metals, measured by three-dimensional computed X-ray tomography and digital volume correlation", *Acta Materialia*, 82, 468-482.

Mostafavi, M., McDonald, S. A., Mummery, P. M. and Marrow, T. J. (2013b), "Observation and quantification of three-dimensional crack propagation in poly-granular graphite", *Engineering Fracture Mechanics*, 110, 410-420.

Nightingale, R. E. (1963), "Nuclear graphite", *J Nucl Mater*, 10, 263-264.

Ouagne, P., Neighbour, G. B. and McEnaney, B. (2004), "Controlled crack growth in an oxidized nuclear grade graphite", *Journal of Physics D: Applied Physics*, 37, 3192.

Preston, S. D. (1988), "Variation of material properties within a single brick of the Heyshal2/Torness moderator graphite", Springfields Nuclear Power Development Laboratories, .

Preston, S. D. and Marsden, B. J. (2006), "Changes in the coefficient of thermal expansion in stressed Gilsocarbon graphite", *Carbon*, 44, 1250-1257.

Sánchez-Arévalo, F. M. and Pulos, G. (2008), "Use of digital image correlation to determine the mechanical behavior of materials", *Mater Charact*, 59, 1572-1579.

Taylor, R., Brown, R. G., Gilchrist, K., Hall, E., Hodds, A. T., Kelly, B. T. and Morris, F. (1967), "The mechanical properties of reactor graphite", *Carbon*, 5, 519-531.

Triconnet, K., Derrien, K., Hild, F. and Baptiste, D. (2009), "Parameter choice for optimized digital image correlation", *Optics and Lasers in Engineering*, 47, 728-737.

Tucker, M. O., Rose, A. P. G. and Burchell, T. D. (1986), "The fracture of polygranular graphites", *Carbon*, 24, 581-602.

Wendland, H. (2004), "Scattered data approximation", Cambridge university press, 17.